

Adsorption of zinc on bed sediment of River Hindon: adsorption models and kinetics

C.K. Jain^{a,*}, D.C. Singhal^b, M.K. Sharma^a

^a National Institute of Hydrology, Environmental Hydrology Division, Jal Vignyan Bhavan, Roorkee 247667, India

^b Indian Institute of Technology, Roorkee 247667, India

Received 24 December 2003; received in revised form 31 August 2004; accepted 1 September 2004

Abstract

The paper presents a study of zinc adsorption using the experimental data on bed sediments of River Hindon in western Uttar Pradesh (India). The effect of various operating variables, viz., initial concentration, solution pH, sediment dose, contact time, and particle size, have been studied. The optimum contact time needed to reach equilibrium was of the order of 60 min and was independent of initial concentration of zinc ions. The extent of adsorption increased with an increase of pH. Furthermore the adsorption of zinc increases with increasing adsorbent doses and decreases with the adsorbent particle size. The content of iron, manganese and organic matter in various fraction of sediment decreases with increasing particle size indicating the possibility of the two geochemical phases to act as the active support material for the adsorption of zinc ions. The adsorption data follows both Langmuir and Freundlich adsorption models. Isotherms were used to determine thermodynamic parameters, viz., free energy change, enthalpy change and entropy change. The negative values of free energy change indicate spontaneous nature of the adsorption while positive values of enthalpy change suggest the endothermic nature of the adsorption of zinc on bed sediment of the River Hindon. The positive values of entropy change indicate randomness at the solid/solution interface.

© 2004 Elsevier B.V. All rights reserved.

Keywords: Adsorption models; Thermodynamics; Zinc; Sediments; Kinetics

1. Introduction

The presence of heavy metals has long been used to determine the extent of pollution in a given area. Many rivers in densely populated areas contain anomalously high concentration of metals. The metal concentrations in river water generally vary with flow as well as sediment concentrations. The heavy metal load of sediments often reaches such high levels that its sudden desorption pose a great danger [1]. Therefore sorption and desorption processes influence the water quality to a considerable extent. Occasional transport of sediment-rich water results in increased heavy metal concentration in rivers. The presence of organic complexes such as humides,

fulvic acids, etc. also accounts for higher level of metals in the sediments due to the formation of organo-metallic complexes.

Pollution from industrial and agricultural sources to a great extent is responsible for high concentration of zinc in river water [2]. This may also be contributed by water distribution system due to leaching of zinc from galvanized pipes. Zinc is an essential element for both animals and men and is necessary for the functioning of various enzyme systems, deficiency of which leads to growth retardation. Low intake of zinc results in retardation of growth, immaturity and anemia, condition known as 'zinc deficiency syndrome'. Symptoms of zinc toxicity in humans include vomiting, dehydration, electrolyte imbalance, abdominal pain, nausea lethargy, dizziness and lack of muscular coordination. Zinc imparts undesirable, bitter astringent taste to water at levels above 5.0 mg/L [3]. Toxic concen-

* Corresponding author. Tel.: +91 1332 272906x249; fax: +91 1332 272123.

E-mail address: ckj@nih.ernet.in (C.K. Jain).

trations of zinc above recommended value cause adverse effect in the morphology of fish by inducing cellular breakdown of gills. Zinc deficiency in human body may also result in infantilism, impaired wound healing and several other diseases.

A number of technologies have been developed to remove toxic metals from water. The most important of these include chemical precipitation, ion exchange, reverse osmosis and adsorption. The suspended and riverbed sediments play an important role in the transport of metals in aquatic systems. The important components of the suspended load for geochemical transport are silt, clay, hydrous iron and manganese oxides and organic matter [1,4]. Generally, the adsorption study for sediment less than 50 μm has been reported widely, while that for the sediment more than 75 μm are few because of little adsorption action [5]. Adsorption properties of the sediments provide valuable information relating to the tolerance of the system to the added heavy metal load.

Despite the wide variability of composition of the sediments depending upon the prevailing conditions, some inherent structural and surface properties favouring heavy metal sorption characterize them. A number of ingredients present in sediments are identified as sorption active compounds and are studied and reported by different authors. Forstner [6] compiled the most association of heavy metals in particulate form in sediments, where he described the active constituents with the nature of association. Jenne [4] discussed the role of clay sized minerals in trace element sorption by soils and sediments. Lion et al. [7] studied the adsorption characteristics of estuarine particulate matter with reference to Fe/Mn oxide and organic surface coatings. Gagnon et al. [8] studied the sorption interactions between trace metals and phenolic substance on suspended clay minerals. Fu and Allen [9] studied the adsorption of cadmium by oxic sediments using a multi-site binding model. The model has been used satisfactorily to predict the extent of adsorption over the pH range 4.5–7.0. Bajracharya et al. [10] studied the effect of zinc and ammonium ions on the adsorption of cadmium on sand and soil and reported that both the ions suppress the adsorption capacity significantly.

Although clay and silt component adsorb metal ions much better than coarser fraction of sediment, one should take into account that most river sediments contain 90–95% sand and only 0–10% clay and silt. Therefore, in river systems with high sand percentage and low clay and silt content, the overall contribution of sand content to adsorption of metal ions could be comparable to or even higher than that of clay and silt fraction [5,11,12]. In the present study, adsorption of zinc on bed sediments of River Hindon has been studied with a view to demonstrate the role of bed sediments in controlling metal pollution. Adsorption data has been analysed with the help of adsorption models to determine the adsorption constants associated with the adsorption process and isotherms have been used to obtain thermodynamic parameters.

2. Study area

The River Hindon is one of the important rivers in western Uttar Pradesh (India), with a basin area of about 7000 km^2 and lies between latitude 28°30' to 30°15'N and longitude 77°20' to 77°50'E. The study area is a part of Indo-Gangetic Plains, composed of Pleistocene and subrecent alluvium. The river originates from Upper Shivaliks (Lower Himalayas) and flows through four major districts, viz., Saharanpur, Muzaffarnagar, Meerut and Ghaziabad in western Uttar Pradesh and covers a distance of about 200 km before joining the River Yamuna downstream of Delhi. The major landuse in the basin is agriculture and there is no effective forest cover. The average annual rainfall is about 1000 mm, major part of which is received during the monsoon period (June to September). The main sources of pollution in River Hindon include municipal wastes from Saharanpur, Muzaffarnagar and Ghaziabad urban areas and industrial effluents of sugar, pulp and paper, distilleries and other miscellaneous industries through tributaries as well as direct outfalls. The physico-chemical characteristics of different effluent drains joining River Hindon and their impact on river water quality has been discussed in an earlier report [13].

3. Experimental methodology

All chemicals used in the study were obtained from Merck, India and were of analytical grade. Deionized water was used throughout the study. All glassware and other containers were thoroughly cleaned and finally rinsed with deionized water several times prior to use.

Freshly deposited sediments from shallow water near the bank of River Hindon at Khaj nawar were collected in polyethylene bags and brought to the laboratory. Samples were taken from the upper 5 cm of the sediments at places where flow rates were low and sedimentation was assumed to occur [14,15].

Textural features of the sediments were observed and a preliminary classification made according to grain-size and distinctive geochemical features. The important geochemical phases for the adsorption process are organic matter, manganese oxides, iron oxides and clays. The contents of manganese oxide and iron oxide were measured as total manganese and total iron, respectively, and extracted from the sediment samples using an acid digestion mixture ($\text{HF} + \text{HClO}_3 + \text{HNO}_3$) in an open system.

Adsorption experiments were conducted in a series of Erlenmeyer flasks of 100 mL capacity covered with a teflon sheet to prevent contamination. Fifty mL of zinc ion solution (200–2000 $\mu\text{g/L}$) was transferred in the flasks together with desired adsorbent doses (W_s in g/L), and placed in a water bath shaker maintained at desired temperature. The pH of the solution was maintained throughout the experiment using dilute HNO_3 and NaOH solutions. The pH was measured before and after the solution had been in contact with the sediment,

Table 1
Characteristics of sediments

Sediment fraction (μm)	Weight (%)	Total Mn (mg/g)	Total Fe (mg/g)	Organic matter (mg/g)
<75	2.2	2.808	112.40	2.067
75–150	20.2	2.250	78.24	1.123
150–210	24.1	1.648	28.04	0.695
210–250	35.7	0.650	13.76	0.547
250–300	6.5	0.258	7.20	0.532
300–425	10.5	0.183	6.84	0.517
425–600	0.8	–	–	–

the difference between the two values was generally less than 0.1 pH unit. Aliquots were retrieved periodically and filtered through 0.45 μm membrane filters. The filters were soaked in dilute (1%, v/v) HNO_3 for 1 h and thoroughly rinsed with deionized water prior to use. The filtrate was analysed for the remaining concentrations of studied metal.

Perkin-Elmer atomic absorption spectrometer (model 3110) was used for determination of concentration of zinc. Average values of five replicates were taken for each determination. Operational conditions were adjusted in accordance with the manufacturer's guidelines to yield optimal determination. Quantification of zinc was based upon calibration curves of standard solutions of zinc ion. These calibration curves were determined several times during the period of analysis. The detection limit for zinc ion was 0.0008 mg/L.

4. Result and discussions

The sediment characteristics of River Hindon is given in Table 1. The sediment has a rather coarse texture, composed of more than 95% sediment of size $>75 \mu\text{m}$ and $<5\%$ silt and clay. The organic content of the sediment was of the order of 0–1%. The background zinc level in the various fractions of the sediments was negligible (below detection limit) in the unpolluted zone, compared to the amount of adsorbate added for the adsorption tests. This confirms the absence of any zinc particulate attached to the sediment particles. The content of iron, manganese and organic matter in various fraction of sediment decreases with increasing particle size indicating the possibility of the two geochemical phases to act as the active support material for the adsorption of zinc ions.

Since the sediment fraction 210–250 μm has comparatively higher weight percentage (i.e. 35.7%), therefore it was considered appropriate to study the comparative adsorption of zinc ions on this fraction and clay and silt fraction ($<75 \mu\text{m}$) to demonstrate the importance of the coarser fraction in controlling metal pollution.

5. Effect of operating variables

5.1. Equilibrium time (t)

The effect of contact time on the adsorption of zinc ions on two particle size of adsorbents is shown in Fig. 1. The asymptotic nature of the plot indicates that there is no appreciable change in the remaining concentration after 60 min. This time is presumed to represent the equilibrium time at which an equilibrium concentration is attained. The equilibrium time was found to be independent of initial concentration. All the further experiments were, thus, conducted for 60 min. Adsorption curves are smooth and continuous leading to saturation, suggesting the possible monolayer coverage of zinc ions on the surface of the adsorbent.

According to Weber and Morris [16], for most adsorption processes, the uptake varies almost proportionately with $t^{1/2}$ rather than with the contact time, t . Therefore, plot of zinc adsorbed, C_t versus $t^{1/2}$, are presented for the two particle sizes of adsorbent in Fig. 1. The plots have same general features, initial curved portion followed by linear portion and a plateau. The initial curved portion is attributed to the bulk diffusion, the linear portion to the intraparticle diffusion and the

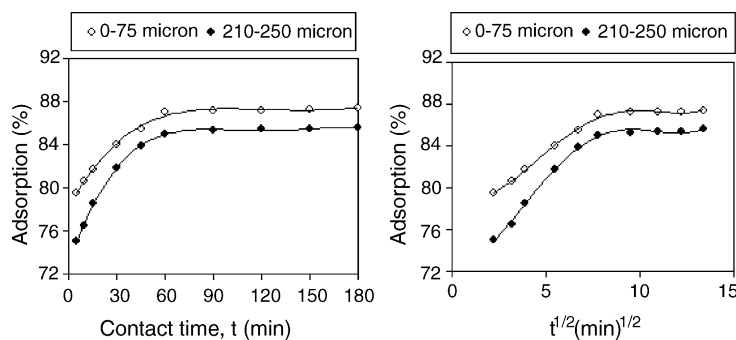


Fig. 1. Effect of contact time (t and $t^{1/2}$) on percent adsorption of zinc ions.

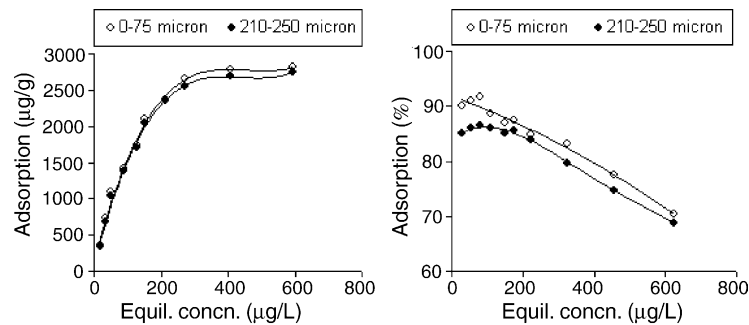


Fig. 2. Adsorption of zinc ions on bed sediments at different concentrations.

plateau to the equilibrium. The experiments were conducted at pH <7.0 to avoid any precipitation of zinc ions.

5.2. Adsorption isotherms

The adsorption isotherms of zinc are shown in Fig. 2. It is evident from the isotherm that there is a linear distribution in the range 0–1000 µg/L. Further, for the same equilibration time, the adsorption of zinc is higher for greater values of initial concentration of zinc ions or the percentage adsorption is more for lower concentration of zinc and decreases with increasing initial concentration. This may be due to the fact that for a fixed adsorbent dose, the total available adsorption sites are limited thereby adsorbing almost the same amount of adsorbate thus resulting in a decrease in percentage uptake of the adsorbate corresponding to an increased initial adsorbate concentration.

A comparison of two plots reveals that the affinity of zinc is more for <75 µm fraction, i.e., clay and silt as compared to coarser fraction. This may be attributed to the fact that <75 µm fraction contain more iron and manganese content than that of 210–250 µm fraction indicating the possibility of association of these substrate with clay and silt particles. These findings reveal the possible role of clay and silt components as active support for the adsorption of zinc ions. The clay and silt constitutes <5% of the total sediment load and therefore, comparing the two weight percentage of the two fractions and their corresponding adsorption capacities for zinc ions, it is clear that the contribution of coarser sediment is more in controlling metal pollution as compared to clay and silt fraction.

5.3. Effect of pH

The effect of pH on the adsorption of zinc ions is shown in Fig. 3 for a fixed initial concentration of zinc ions (1000 µg/L) and adsorbent dose of 0.5 g/L at a particle size of 0–75 and 210–250 µm. Experiments could not be performed at higher pH values due to low solubility of metal ions. A general increase in adsorption with increasing pH of solution has been observed up to the pH value of 6.0 for both the fractions of the sediment. From the results, it is evident that the pH for maximum uptake of zinc ions is 6.0. Further, it is apparent

that the adsorption of zinc rises from 7.5% at pH 2.0 to 86.9% at pH 6.0 in the case of clay and silt fraction (0–75 µm) and from 5.2% at pH 2.0 to 84.8% at pH 6.0 in the case of coarser sediment fraction (210–250 µm). Almost similar behaviour with pH was reported by many authors [17–23] on various adsorbents.

5.4. Effect of adsorbent dose (W_s)

The effect of adsorbent dose on the adsorption of zinc ions is shown in Fig. 4 for a fixed initial concentration of 1000 µg/L. It is observed that the adsorption of zinc per unit weight of adsorbent decreases with increasing adsorbent load. On the other hand, percent adsorption increases from 86.9 to 93.0% for the 0–75 µm fraction with increasing adsorbent load from 0.5 to 2.5 g/L.

5.5. Effect of particle size (d_p)

The effect of particle size of adsorbent on the adsorption of zinc is shown in Fig. 4. These plots reveal that for a fixed adsorbent dose, the adsorption of zinc is higher for smaller adsorbent size. Further, it is observed that the percentage adsorption decreases with increasing geometric mean of adsorbent size. This is because, adsorption being a surface phenomenon, the smaller particle sizes offered comparatively larger surface area and hence higher adsorption occurs at equilibrium. Similar trend with adsorbent dose and size was also reported by other workers [5,11,12,24,25] for the uptake of metal ions on various adsorbents. The higher

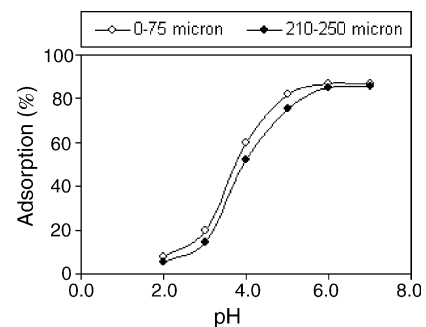


Fig. 3. Effect of pH on percent adsorption of zinc ions.

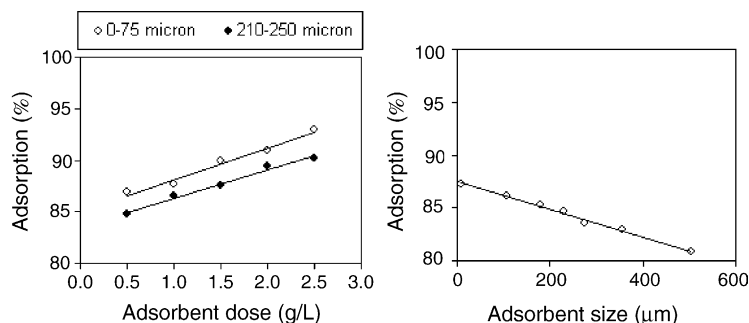


Fig. 4. Effect of adsorbent dose and adsorbent size on percent adsorption of zinc ions.

content of iron and manganese in the 0–75 μm sediment fraction also accounts for higher adsorption in this fraction, which is the main driving force for the adsorption of zinc ions.

6. Adsorption models

In general, the adsorption isotherm describes how adsorbates will interact with adsorbents and so is critical in optimizing the use of adsorbent. Adsorption data for wide range of adsorbate concentrations are most conveniently described by adsorption models, such as the Langmuir or Freundlich isotherm, which relate adsorption density q_e (metal uptake per unit weight of adsorbent) to equilibrium adsorbate concentration in the bulk fluid phase, C_e . The adsorption models have been used to determine the mechanistic parameters associated with the adsorption process.

6.1. Langmuir model

Langmuir's isotherm model suggests that uptake occurs on homogeneous surface by monolayer sorption without interaction between sorbed molecules. The model assumes uniform energies of adsorption onto the surface and no transmigration of adsorbate in the plane of the surface. The linear form of Langmuir isotherm equation is represented by the following equation [26]:

$$\frac{1}{q_e} = \frac{1}{Q^0} + \frac{1}{bQ^0C_e} \quad (1)$$

where q_e is the amount adsorbed at equilibrium time ($\mu\text{g/g}$), C_e is the equilibrium concentration of the adsorbate ions ($\mu\text{g/L}$), and Q^0 and b are Langmuir constants related to maximum adsorption capacity (monolayer capacity) and energy of adsorption, respectively. When $1/q_e$ is plotted against $1/C_e$, a straight line with slope $1/bQ^0$ and intercept $1/Q^0$ is obtained (Fig. 5), which shows that the adsorption of zinc follows Langmuir isotherm model. The Langmuir parameters, Q^0 and b , are calculated from the slope and intercept of the graphs and are given in Table 2. These values may be used for comparison and correlation of the sorptive properties of the sediments.

6.2. Freundlich model

The Freundlich equation has been widely used and is applicable for isothermal adsorption. This is a special case for heterogeneous surface energies in which the energy term, b , in the Langmuir equation varies as a function of surface coverage, q_e , strictly due to variations in heat of adsorption [27]. The Freundlich equation has the general form [28]:

$$q_e = K_F C_e^{1/n} \quad (2)$$

The Freundlich equation is basically empirical but is often useful as a means for data description. Data are usually fitted to the logarithmic form of the equation:

$$\log q_e = \log K_F + \frac{1}{n} \log C_e \quad (3)$$

where q_e is the amount adsorbed ($\mu\text{g/g}$), C_e is the equilibrium concentration of the adsorbate ions ($\mu\text{g/L}$), and K_F and n are Freundlich constants related to adsorption capacity and adsorption intensity, respectively (Table 3). When $\log q_e$ is plotted against $\log C_e$, a straight line with slope $1/n$ and intercept $\log K_F$ is obtained (Fig. 5). This reflects the satisfaction of Freundlich isotherm model for the adsorption of zinc ions. The intercept of line, $\log K_F$, is roughly an indicator of the adsorption capacity and the slope, $1/n$, is an indicator of adsorption intensity [29]. The Freundlich parameters for the adsorption of zinc are also given in Table 2. It is evident from this data that the surface of the bed sediments of the River Hindon is made up of small heterogeneous adsorption

Table 2
Langmuir parameters for adsorption of zinc ions

Sediment fraction (μm)	Adsorption maxima Q^0 (mg/g)	Binding energy constant b ($\text{mg/L})^{-1}$
0–75	5.0	4.338
210–250	12.5	0.974

Table 3
Freundlich parameters for adsorption of zinc ions

Sediment fraction (μm)	Adsorption capacity K_F (mg/g)	Adsorption intensity $1/n$
0–75	0.088	0.593
210–250	0.046	0.690

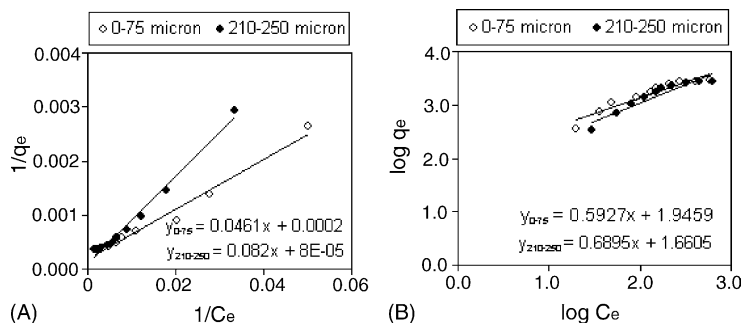


Fig. 5. Graphical representation of adsorption isotherms: (A) Langmuir isotherm and (B) Freundlich isotherm.

patches which are very much similar to each other in respect of adsorption phenomenon [25].

7. Adsorption kinetics

7.1. Thermodynamic parameters

The effect of temperature on adsorption of zinc onto bed sediment of River Hindon is depicted in Fig. 6 for a fixed adsorbent dose of 0.5 g/L and initial zinc concentration of 1000 $\mu\text{g/L}$. The temperature range used in the study was from 20 to 40 °C. Adsorption increased with increase in temperature, which may be mainly due to the increase in number of active sites caused by the breaking of some bonds. Thermodynamic parameters such as free energy change (ΔG°), enthalpy change (ΔH°) and entropy change (ΔS°) were determined using the following equation [30–32].

$$\Delta G^\circ = -RT \ln K_c \tag{4}$$

$$\Delta G^\circ = \Delta H^\circ - T \Delta S^\circ \tag{5}$$

where ΔG° is the change in free energy, kJ/mol; ΔH° the change in enthalpy, kJ/mol; ΔS° the change in entropy, J/mol/K; T the absolute temperature, K; R the gas constant = 8.314×10^{-3} ; and K_c the equilibrium constant. This may be defined as:

$$K_c = \frac{C_{Ae}}{C_e} \tag{6}$$

where C_{Ae} and C_e are the equilibrium concentration ($\mu\text{g/L}$) of the metal ion on the adsorbent and in the solution respectively.

From Eqs. (4) and (5), it can be rewritten as:

$$\log K_c = \frac{\Delta S^\circ}{2.303R} - \frac{\Delta H^\circ}{2.303RT} \tag{7}$$

When $\log K_c$ is plotted against $1/T$, a straight line with slope $\Delta H^\circ/2.303R$ and intercept $\Delta S^\circ/2.303R$ is obtained (Fig. 7). The values of ΔH° and ΔS° were obtained from the slope and intercept of the van't Hoff plots of $\log K_c$ versus $1/T$ (Fig. 7). The thermodynamic parameters for the adsorption process are given in Table 4.

Positive values of ΔH° suggest the endothermic nature of the adsorption of zinc on bed sediment of Hindon. The negative values of ΔG° indicate the feasibility of the process and indicate spontaneous nature of the adsorption. However, the negative value of ΔG° decreased with an increase in temperature, indicating that the spontaneous nature of adsorption of zinc is inversely proportional to the temperature. The positive values of ΔS° show the increased randomness at the solid/solution interface during the adsorption process. A positive entropy of adsorption also reflects the affinity of the adsorbent for zinc ion. Similar findings were also observed by Srivastava et al. [24] and Namasivayam and Ranganathan [33]. The adsorbed water molecules, which are displaced by the adsorbate species, gain more translational energy than is lost by the adsorbate ions, thus allowing the prevalence of randomness in the system. Enhancement of adsorption capacity of adsorbent at higher temperatures may be attributed to the

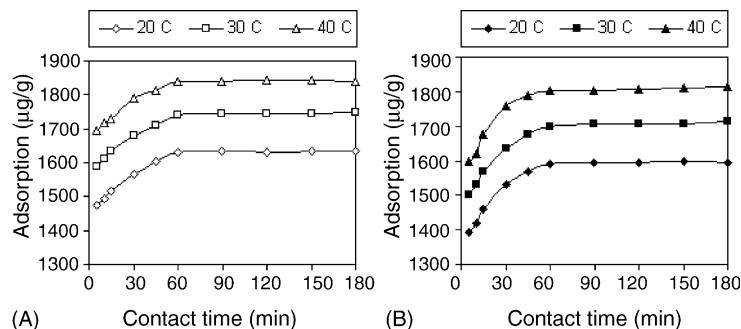


Fig. 6. Effect of contact time and temperature on adsorption of zinc ions: (A) 0–75 μm fraction and (B) 210–250 μm fraction.

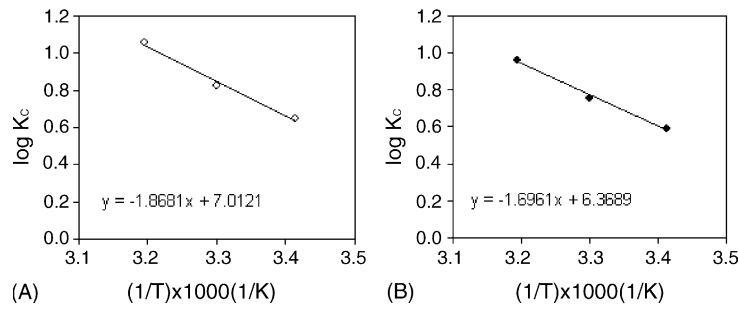


Fig. 7. Van't Hoff plot for adsorption of zinc ions: (A) 0–75 μm fraction and (B) 210–250 μm fraction.

Table 4

Thermodynamic parameters for the adsorption of zinc ions

Sediment fraction (μm)	Temperature ($^{\circ}\text{C}$)	K_c	ΔG° (kJ/mol)	ΔH° (kJ/mol)	ΔS° (kJ/mol)
0–75	20	4.4335	−3.6297	35.770	134.30
	30	6.6920	−4.7899		
	40	11.346	−6.3217		
210–250	20	3.878	−3.3027	32.470	121.90
	30	5.667	−4.3710		
	40	9.101	−5.7479		

enlargement of pore size and/or activation of the adsorbent surface [34].

7.2. Adsorption dynamics

The rate constant of adsorption is determined using Lagergren first-order rate expression:

$$\log(q_e - q) = \log q_e - \frac{k_{ad}}{2.303}t \quad (8)$$

where q and q_e are amounts of metal adsorbed ($\mu\text{g/g}$) at time, t (min) and at equilibrium, respectively and k_{ad} is the Lagergren rate constant for adsorption (1/min). The straight line plots of $\log(q_e - q)$ versus t for different concentrations (Fig. 8) and temperatures (Fig. 9) indicate the applicability of the above equation. Values of k_{ad} were calculated from the slope of the linear plots and are presented in Tables 5 and 6 for different concentrations and temperatures, respectively. The rate constants were higher at higher temperatures. Similar findings were also observed by Namasivayam and Ranganathan [33].

7.3. Intraparticle diffusion

The rate constant for intraparticle diffusion (k_{id}) is given by Weber and Morris [35]:

$$q = k_{id}t^{1/2} \quad (9)$$

where q is the amount adsorbed ($\mu\text{g/g}$) at time, t (min). Plots of q versus $t^{1/2}$ are shown in Figs. 10 and 11 for different initial concentrations and temperatures, respectively. All the plots have the same general features, initial curved portion followed by linear portion and a plateau. The initial curved portion is attributed to the bulk diffusion, the linear portion to the intraparticle diffusion and the plateau to the equilibrium. This indicates that transport of zinc ions from the solution through the particle solution interface, into the pores of the particle as well as the adsorption on the available surface of sediment are both responsible for the uptake of zinc ions. The deviation of the curves from the origin also indicates that intraparticle transport is not the only rate limiting step. The values of rate constants (k_{id}) were obtained from the slope of the linear portion of the curves for each concentration of

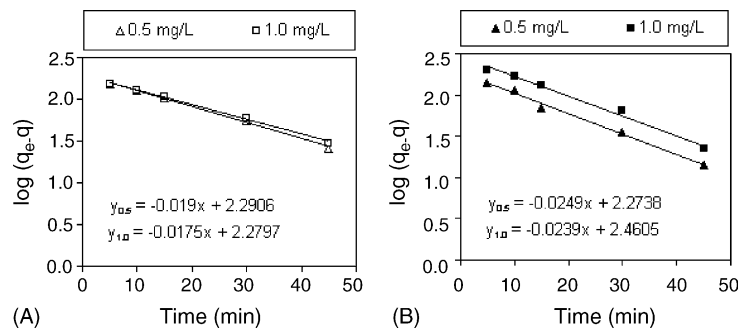


Fig. 8. Lagergren plots at different initial concentrations: (A) 0–75 μm fraction and (B) 210–250 μm fraction.

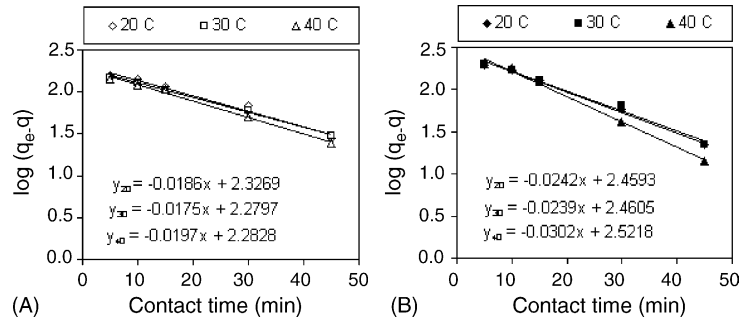


Fig. 9. Lagergren plots at different temperatures: (A) 0–75 μm fraction and (B) 210–250 μm fraction.

Table 5
Rate constants at different concentrations

Sediment fraction (μm)	Concentration of zinc (μg/L)	Lagergren rate constant k_{ad} (1/min)	Intraparticle rate constant k_{id} (μg/g/min ^{1/2})
0–75	500	4.38×10^{-2}	14.000
	1000	4.03×10^{-2}	17.770
210–250	500	5.74×10^{-2}	17.144
	1000	5.50×10^{-2}	23.125

Table 6
Rate constants at different temperatures

Sediment fraction (μm)	Temperature (°C)	Lagergren rate constant k_{ad} (1/min)	Intraparticle rate constant k_{id} (μg/g/min ^{1/2})
0–75	20	4.28×10^{-2}	13.125
	30	4.03×10^{-2}	15.625
	40	4.54×10^{-2}	18.125
210–250	20	5.57×10^{-2}	25.455
	30	5.50×10^{-2}	26.364
	40	6.96×10^{-2}	27.273

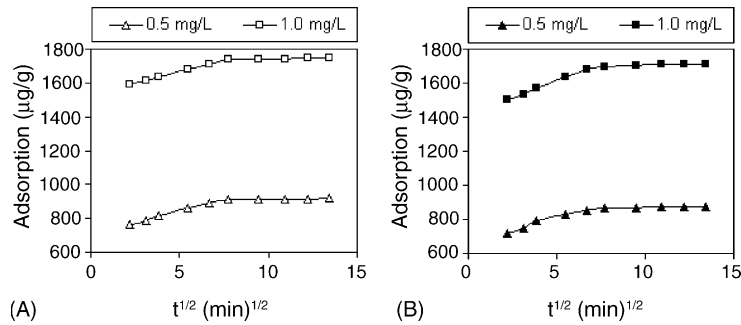


Fig. 10. Intraparticle diffusion plots at different initial concentrations: (A) 0–75 μm fraction and (B) 210–250 μm fraction.

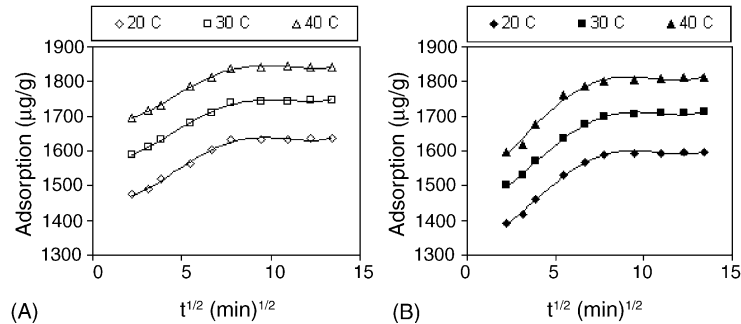


Fig. 11. Intraparticle diffusion plots at different temperatures: (A) 0–75 μm fraction and (B) 210–250 μm fraction.

metal ions (Table 5) and temperatures (Table 6). The value of intraparticle rate constant (k_{id}) was higher at higher concentration. Increasing temperature slightly improved the k_{id} , but did not have any significant effect. Similar findings were also observed by Namasivayam and Ranganathan [33].

8. Conclusion

It is concluded from the study that though zinc ions have more affinity for the fine fraction of the sediment, but the overall contribution of coarser fraction to adsorption is more as compared to clay and silt fraction. The adsorption data suggests that the pH of the solution is the most important parameter in the control of metal pollution. The percentage adsorption increases with increasing adsorbent doses, and as such removal increases with decreasing size of the adsorbent material. The two important geochemical phases, iron and manganese oxide, also play an important role in the adsorption process. The content of iron in the sediment fractions was found to be relatively higher indicating the possibility of presence of iron minerals other than hydroxides. The equilibrium data describe the Langmuir and Freundlich isotherm models satisfactorily. The kinetic data suggest that the adsorption of zinc on bed sediments is an endothermic process, which is spontaneous at low temperature. The uptake of zinc is controlled by both bulk as well as intraparticle diffusion mechanisms. The results of the experimental study obtained from this study are highly useful and may be extended for other rivers with coarser sediments.

References

- [1] W. Salomons, U. Forstner, *Metals in the Hydrocycle*, Springer, Berlin, 1984.
- [2] V. Novotny, G. Chesters, Van Nostrand Reinhold Company, New York, 1981.
- [3] WHO, *Guidelines for Drinking Water Quality*, vol. 2, 2nd ed., WHO, Geneva, 1996.
- [4] E.A. Jenne, in: W. Chappel, K. Petersen (Eds.), *Symposium on Molybdenum*, vol. 2, Marcel Dekker, New York, 1976, pp. 425–453.
- [5] C.K. Jain, I. Ali, *Hydrol. Process.* 14 (2000) 261–270.
- [6] U. Forstner, in: H.L. Golterman (Ed.), *Interaction between Sediments and Freshwater*, Wageningen, Pudoc/Junk B.V. Publ., The Hague, 1977, pp. 94–103.
- [7] L.W. Lion, R.S. Altmann, J.O. Leckie, *Environ. Sci. Technol.* 16 (1982) 660–666.
- [8] C. Gagnon, M. Arnac, J.R. Brindle, *Water Res.* 26 (1992) 1067–1072.
- [9] G. Fu, H.E. Allen, *Water Res.* 26 (1992) 225–233.
- [10] K. Bajracharya, D.A. Barry, S. Vigneswaran, A.D. Gupta, in: V.P. Singh, B. Kumar (Eds.), *Water Quality Hydrology*, vol. 3, Kluwer Academic Publishers, The Netherlands, 1996, pp. 19–26.
- [11] C.K. Jain, D. Ram, *Water Res.* 31 (1997) 154–162.
- [12] C.K. Jain, D. Ram, *Hydrol. Sci. J.* 42 (1997) 713–723.
- [13] C.K. Jain, M.K. Sharma, *Hydro-chemical Studies of Hindon River*, Technical Report, CS(AR)21/98-99, National Institute of Hydrology, Roorkee, India, 1999.
- [14] H. Sakai, Y. Kojima, K. Saito, *Water Res.* 20 (1986) 559–567.
- [15] V. Subramanian, R.V. Griken, D.L. Vant, *Environ. Geol. Water Sci.* 9 (1987) 93–103.
- [16] W.J. Weber Jr., J.C. Moris, *J. Sanit. Eng. Div. ASCE* 89 (1963) 31–60.
- [17] M.M. Benzamin, J.O. Lackie, in: R.A. Baker (Ed.), *Contaminants and Sediments*, vol. 2, 1980, pp. 305–322.
- [18] T.H. Christensen, *Water Air Soil Pollut.* 21 (1984) 105–114.
- [19] J.O. Wiley, P.O. Nelson, *J. Environ. Eng. ASCE* 110 (1984) 226–243.
- [20] B. Palheiros, A.C. Duarte, J.P. Oliveira, A. Hall, *Water Sci. Technol.* 21 (1989) 1873–1876.
- [21] H. Farrah, W.F. Pickering, *Aust. J. Chem.* 29 (1976) 1167–1176.
- [22] H. Farrah, W.F. Pickering, *Aust. J. Chem.* 29 (1976) 1177–1184.
- [23] A. Netzer, P. Wilkinson, *Proceedings of the 29th Waste Conference*, Purdue, 1976, pp. 841–845.
- [24] S.K. Srivastava, V.K. Gupta, D. Mohan, *J. Environ. Eng. ASCE* 123 (1997) 461–468.
- [25] M. Ajmal, A.H. Khan, S. Ahmad, A. Ahmad, *Water Res.* 32 (1998) 3085–3091.
- [26] I. Langmuir, *J. Am. Chem. Soc.* 40 (1918) 1361–1403.
- [27] A.W. Adamson, *Physical Chemistry of Surfaces*, 2nd ed., Interscience Publishers Inc., New York, 1967.
- [28] H. Freundlich, *Colloid and Capillary Chemistry*, Methuen, London, 1926.
- [29] W.J. Weber Jr., *Physico-Chemical Processes for Water Quality Control*, John Wiley and Sons Inc., New York, NY, 1972.
- [30] A.K. Singh, D.P. Singh, K.K. Pandey, V.N. Singh, *J. Chem. Technol. Biotechnol.* 42 (1988) 39–49.
- [31] G.C. Catena, F.V. Bright, *Anal. Chem.* 61 (1989) 905–909.
- [32] L.K. Fraiji, D.M. Hayer, T.C. Werner, *J. Chem. Educ.* 69 (1992) 205–215.
- [33] C. Namasivayam, K. Ranganathan, *Water Res.* 29 (1995) 1737–1744.
- [34] P.P. Vishwakarma, K.P. Yadava, V.N. Singh, *Pertanika* 12 (1989) 357–366.
- [35] W.J. Weber Jr., J.C. Moris, *Advances in Water Pollution Research*, Proceedings of the 1st International Conference on Water Pollution Research, vol. 2, Pergamon Press, Oxford, 1962, p. 231.